Salidroside Alleviates Oxidative Stress and Apoptosis via AMPK/Nrf2 Pathway in DHT-induced Human Granulosa Cell Line KGN

Rui Ji
Renmin Hospital of Wuhan University: Wuhan University Renmin Hospital
Fang-yuan Jia
Central China Fuwai Hospital of Zhengzhou University
Xin Chen
Renmin Hospital of Wuhan University: Wuhan University Renmin Hospital
Ze-hao Wang
Renmin Hospital of Wuhan University: Wuhan University Renmin Hospital
Wen-yi Jin
Renmin Hospital of Wuhan University: Wuhan University Renmin Hospital
Jing Yang (dryangjing@whu.edu.cn)
Renmin Hospital of Wuhan University: Wuhan University Renmin Hospital

Research

Keywords: Salidroside, Polycystic ovary syndrome, oxidative stress, Nrf2, AMPK

Posted Date: September 2nd, 2021

DOI: https://doi.org/10.21203/rs.3.rs-842159/v1

Version of Record: A version of this preprint was published at Archives of Biochemistry and Biophysics on November 1st, 2021. See the published version at https://doi.org/10.1016/j.abb.2021.109094.

Abstract

Background: In the past few years, emerging evidence established persistent oxidative stress to be a key player in the pathogenesis of polycystic ovary syndrome (PCOS). Particularly, it damages the function of granulosa cells, and thus hinders the development of follicles. The present study aimed to explore and establish the protective effects of salidroside on dihydrotestosterone (DHT)-induced Granulosa-like tumor cell line (KGN), mediated via antioxidant mechanisms.

Methods: KGN cells were treated with DHT as a PCOS cell model, and then incubated with salidroside in different concentrations. Apoptosis and reactive oxygen species (ROS) accumulation were assessed by flow cytometry, mitochondrial membrane potential depolarization and the nuclear translocation of Nrf2 were detected by immunofluorescence staining, and the level of apoptosis-related proteins and antioxidant proteins was assessed by western blotting.

Results: Salidroside partly reversed DHT mediated effects, via stimulation of nuclear factor erythroid 2-related factor 2 (Nrf2) signaling pathway and the downstream antioxidant proteins heme oxygenase-1(HO-1) and quinine oxidoreductase 1(NQO1). Additionally, knockdown of Nrf2 resulted in a deterioration in DHT-induced oxidative stress and apoptosis. It partly moderated the protective effects of salidroside as well. Mechanistically, AMPK was identified to be the upstream signaling involved in salidroside-induced Nrf2 activation, as silencing of AMPK partly prevented the upregulation of Nrf2 and the downstream proteins HO-1 and NQO1.

Conclusion: The present study is the first to effectively demonstrate the inhibitory effect of salidroside on DHT-stimulated oxidative stress and apoptosis in KGN cells, which was dependent on Nrf2 activation that involved AMPK.

Introduction

Granulosa cells constitute the cell layer present in the follicles that interact with oocytes and mediate the metabolism, transport of materials, and signal transduction in oocytes. Additionally, these cells play a crucial role in follicular growth, proliferation, differentiation, atresia/ovulation, and formation of the corpus luteum[1]. Several female reproductive endocrine diseases related to hormonal changes and follicular development, such as premature ovarian failure and polycystic ovary syndrome (PCOS), are associated with abnormal changes in granulosa cells, which are known to be involved in the disease developmental process[2, 3]. PCOS is the most common female reproductive endocrine disease; however, the pathogenesis of the disease remains unclear. Excessive androgen has been proved to play a vital role in the pathogenesis of PCOS. In particular, higher androgen levels result in insulin resistance and obesity and ultimately affect the function of granulosa cells and follicle development via complex mechanisms[4]. Granulosa-like tumor cell line (KGN) possesses steroidogenesis capability and is considered to be a reliable cell model to gain mechanistic insights into human granulosa cells[5]. In recent times, DHT-induced KGN cells have been widely used for *in vitro* studies involving PCOS[6, 7].

In general, oxidative stress refers to a series of adaptive reactions caused by an imbalance between the oxidants and antioxidants. During this process, excessive reactive oxygen species (ROS) cannot be eliminated in time, which get accumulated and interfere with the normal redox state of the cells. Several previous studies have reported the existence of oxidative stress in PCOS. Interestingly, the levels of oxidative stress markers, such as 8-OHDG and MDA, have been reported to be elevated in the serum and follicular fluid of PCOS patients[8, 9]. An increase in oxidative stress has been proved to be related to the progression of PCOS and the associated complications, such as T2DM and cardiovascular diseases[10]. Besides this, oxidative stress also leads to the apoptosis of granulosa cells, thereby obstructing the development and maturation of oocytes[11]. The antioxidant systems respond to the oxidative damage, incurred by the inevitable generation of ROS, via a series of signaling pathways. Nuclear factor (erythroid-derived 2)-like 2 (NRF2) has been identified as one of the main transcription factors associated with the oxidative stress response[12]. It belongs to the Cap'n'Collar (CNC) subfamily of basic leucine zipper (bZIP) transcription factors. In particular, Nrf2 consists of seven conserved NRF2-ECH homology (Neh) domains with different functions, which modulate the stability of Nrf2 and contribute to its central role in the redox system. Nrf2 activity is precisely regulated by Kelch-like-ECH-associated protein 1 (Keap1). In the steady-state, Nrf2 is anchored in the cytoplasm at a low basal protein level by Keap1, which binds NRF2 via its C-terminal domain, resulting in Keap1-Cullin (CUL) 3-RING-box protein-mediated ubiquitination of NRF2 and degradation by the 26S proteasome[13]. Under oxidative stress, Keap1 is inactivated, and the newly synthesized Nrf2 escapes from Keap1 and translocate quickly into the nuclear region, where it induces the transcription of an array of antioxidant genes, such as heme oxygenase 1 (HO-1), quinine oxidoreductase 1 (NQO1), and reduced form of nicotinamide adenine dinucleotide phosphate (NADPH)[14]. However, the underlying mechanism involved in the activation of Nrf2 and disassociation from the Keap1-Nrf2 complex remains elusive. Several previous studies have testified that Nrf2 and its downstream protein like HO-1 could be enhanced by the activation of mitogen-activated protein kinase (MAPK) and phosphatidylinositol-3-kinase (PI3K)/Akt-dependent phosphorylation[15, 16]. AMP-activated protein kinase (AMPK) is a heterotrimeric enzyme that plays a pivotal role in the maintenance of redox homeostasis[17]. A recent study reported that AMPK promoted the detachment of Nrf2-Keap1 complex and nuclear transcription in sodium fluoride (NaF)-stimulated microglia[18].

Salidroside is a phenylpropanoid glycoside compound, extracted from the dried roots or whole plant of *Rhodiola rosea*, which possesses antioxidant properties (Fig. 1A). In fact, several studies have previously established that salidroside alleviated oxidative stress injury in the cardiovascular system, endocrine disease, neurodegenerative disease, [19–21]etc. Moreover, a recent study reported that salidroside alleviated HUVECs cell injury, induced by oxidative stress, via activation of the Nrf2 signaling pathway[22]. However, very limited information is available regarding the role of salidroside on oxidative stress in PCOS.

The present study aimed to explore whether salidroside can incur a protective effect on suppressing the oxidative stress and apoptosis in DHT-induced KGN, and thus unravel the underlying mechanism responsible for its functions in KGN cells

Materials And Methods

Reagents

Salidroside (#HY-N0109) and Compound C (#HY-13418A) were purchased from MedChemExpress (China); DHT (#S4757) was purchased from Selleck (China), and AMPK siRNA (#sc45312) and negative control siRNA (#sc-37007) were purchased from Santa Cruz Biotech. Nrf2 siRNA and RNATransMate (#E607402) was purchased from Sangon Biotech (China). The nuclear and cytoplasmic extraction reagent (#78833) was obtained from ThermoFisher (USA). The Mitochondrial Membrane Potential Assay Kit with JC-1 (#C2006), Annexin V-PE Apoptosis Detection Kit (#C1065L), and Cell Counting Kit-8 (CCK-8; #C0037) were obtained from Beyotime Biotechnology (China).

Cell culture and treatment

The KGN cells were provided by the RIKEN BioResource Research Centre (Tsukuba, #RCB1154, Japan). The cell line was cultured in DMEM/F12 medium (Gibco, #11320033, USA) in the presence of 10% FBS (Gibco, #10100, USA) and 1% PS (Servicebio, #G4003-100ML, China) at 37°C under 5% CO_2 atmosphere. The KGN cells were then treated with DHT (500 nM) as a PCOS cell model, which been used in reveral studies[3, 7]. To detect the effects of salidroside, the KGN cells were incubated with salidroside at different concentrations for 24 h.

Cell viability assay

Cell viability was assessed by using the Cell Counting Kit-8 (CCK-8) assay (Beyotime Biotechnology, #C0037, China). The KGN cells were seeded in 96-well flat-bottomed plates at 3×10^3 per well, treated with DHT, low or high doses of salidroside and incubated for 24 h or 48 h, followed by incubation with cck8 (10 μL/well) for 1.5 h, and the absorbance was read at 450 nm on a microplate reader (Perkin Elmer, USA).

Cell transfection

The KGN cells were cultured at the density of 70–90%, and then AMPK siRNA, Nrf2 siRNA, or the negative control siRNA were transfected with the RNA TransMate (Sangon Biotech, #E607402, China) to silence the AMPK and Nrf2 according to the manufacturer's protocol. Next, the cells were incubated for 48 h before testing. The siRNA sequence of Nrf2 was 5'-UUGUGUUUAGUGAAAUGCCGG-3' (Nrf2 siRNA-1), 5'-UAUAUCCCGAAUUAAUGCAAG-3' (Nrf2 siRNA-2), and 5'-UUGCCAUCUCUUGUUUGCUGC-3' (Nrf2 siRNA-3).

ROS analysis

ROS was detected with the ROS Assay Kit (Beyotime Biotechnology, #S0033S, China). The KGN cells were digested by Trypsin–EDTA (0.25%) (Gibco Life Technologies, #25200056, USA) and resuspended in a medium with 5 μM dihydroethidium (DHE). After 30 min of incubation in dark at 37°C, the KGN cells

were washed with phosphate-buffered saline (PBS; Gibco Life Technologies, #10010023, USA), and the production of ROS was assessed by flow cytometry (Beckman , BC43326, USA).

Detection of cell apoptosis

Apoptosis of the KGN cells was detected with the Annexin V-PE Apoptosis Detection Kit (Beyotime Biotechnology, #C1065L). After treatment, the KGN cells were collected with 2.5% trypsin (Gibco Life Technologies, #15090046, USA) and washed twice with PBS. Next, 0.5 mL of the binding buffer was added to resuspend the KGN cells. Then, the resuspended cells were incubated with 5 μL of annexin V-FITC and 10 μL of propidium iodide (PI) in the dark at 37℃ for 15 min. The percentage of apoptotic KGN cells was then calculated by flow cytometry.

Cell immunofluorescence staining

The KGN cells were seeded into a 6-well plate and fixed with 4% paraformaldehyde for 5 min, after which 0.2% Triton X-100 in PBS was used for permeation and 10% normal goat serum was used to block the cells. Then, the cells were incubated with an anti-Nrf2 antibody (1:200; Abcam, #ab137550, UK) overnight at 4℃. The cells were washed with PBS and incubated with a secondary antibody Cy3 conjugated goat anti-rabbit IgG (H+L) for 1 h. 4',6-Diamidino-2-phenylindole (DAPI) was used to label the nuclei. Images were visualized by using a fluorescence microscope (Olympus BX6 with DP72 Camera, Japan).

Mitochondrial Membrane Potential Detection

The Mitochondrial Membrane Potential (MMP) Assay Kit with JC-1 (Beyotime Biotechnology, #C2006, China) was used to analyze the mitochondrial depolarization according to the manufacturer's protocol. The cells were incubated with JC-1 solution for 20 min and then washed with the JC-1 staining buffer. Fluorescence microscopy (Olympus IX73P2F, Japan) was used to analyze the MMP and the corresponding images were assessed by the Image-J software. The red/green fluorescence intensity ratio was used to calculate the changes in the MMP.

Western Blotting

The protein concentrations of the KGN cell lysates were detected by using the BCA protein assay kit (Beyotime Biotechnology, #P0010S, China). The nuclear proteins of the KGN cells were extracted by using the Nuclear and Cytoplasmic Protein Extraction Kits (Beyotime Biotechnology, #P0027, China). The proteins were separated on the SDS-PAGE gels and transferred onto PVDF- membranes. The membranes were blocked with skimmed milk for 2 h and then incubated at 4℃ overnight with primary antibodies against Nrf-2 (1:1000; Abcam, #ab62352, UK), HO-1 (1:2000; Abcam, #ab52947, UK), NQO1 (1:10000; Abcam, #ab80588, UK), AMPK (1:1000; Abcam, #ab133448, UK), phosphor-AMPK (1:1000; Abcam, #ab80039, UK), AKT (1:1000; Proteintech, #10176-2-AP, China), phosphor-AKT (1:2000; Proteintech, #66444-1-Ig, China), ERK (1:2000; Proteintech, #67170-1-Ig, China), phosphor-ERK (1:2000; Cell Signalling Technology, #4370, USA), JNK (1:1000; Proteintech, #24164-1-AP, China), phosphor-JNK (1:1000; Proteintech, #80024-1-RR, China), p38 (1:500; Proteintech, #14064-1-AP, China), phosphor-p38 (1:1000;

Abcam, #ab178867, UK), cleaved caspase-3 (Abcam; 1:500, #ab32042, UK), cleaved caspase-9 (1:1000; Abcam, #ab2324, UK), Bax (1:5000; Proteintech, #50599-2-Ig, China), Bcl2 (1:1000; Proteintech, #12789-1-AP, China), Histone 3 (1:1000; Proteintech, #17168-1-AP, China), and GAPDH (1:20000; Proteintech, #60004-1-Ig, China). Then, horseradish peroxidase-conjugated secondary antibodies were used to incubate the membranes for 1 h, and the bands were visualized by enhanced chemiluminescence (ECL).

Statistical Analysis

All data were analyzed with the GraphPad Prism 8 software. All quantitative data were presented as mean ± standard deviation (SD). Multiple comparisons were used by one-way ANOVA, followed by Tukey's posthoc test. P 0.05 was considered to be statistically significant.

Results

Salidroside improves the survival of DHT-induced KGN cells

To assess the effects of salidroside on KGN cells and determine the appropriate concentration required for its activity, the cytotoxicity of salidroside was evaluated using a cck8 assay. Briefly, KGN cells were treated with different concentrations of salidroside, in 0.2(0, 15 μM, 30 μM, 60 μM, 100 μM, and 120 μM) or 10 FBS(0, 30 μM, 60 μM, 100 μM, 150 μM, and 200μM). The results for the cytotoxicity assay showed that low concentrations of salidroside had a minor side effect on KGN cells. In comparison to this, an increase in salidroside concentration to 120 μM (in serum-deprived condition) and 150 μM (in serum-induced condition) resulted in a decrease in the survival rate of KGN cells (Figure 1B and C). Further, to explore the positive effects of salidroside on KGN cells, the cells were treated with 500 nM DHT as an androgen-induced PCOS cell model. As shown in Figures 1D and E, both the low and high concentrations of salidroside (30 μM or 100 μM) alleviated the symptoms of cell injury induced by DHT treatment in KGN cells at 24 h and 48 h, respectively.

Salidroside alleviates DHT-induced KGN cell apoptosis and oxidative stress

The results for salidroside-mediated survival improvement in KGN cells encouraged the evaluation of the effects of salidroside on ROS levels, mitochondrial membrane potential, and apoptosis in DHT-treated KGN cells. The levels of ROS were found to be significantly higher in DHT-treated KGN cells as compared to the normal group. Further, the addition of low and high concentrations of salidroside (30 μM or 100 μM) partially reversed the observed increase in ROS (Figure 2A and B). Following this, JC-1 fluorescent staining was used to detect the changes in the mitochondrial membrane potential (MMP). As shown in Figures 2C and D, the JC-1 fluorescent probe mainly accumulated in the mitochondrial matrix of the normal cells and emitted red fluorescence. In the case of DHT-treated KGN cells, the JC-1 probe failed to accumulate in the mitochondrial matrix and emitted green fluorescence along with low red fluorescence, which indicated a decrease in MPP. In comparison to these, mitochondrial depolarization was found to be significantly improved in the case of salidroside-treated KGN cells. The results for apoptosis analysis

further indicated that DHT aggravated apoptosis in KGN, however, 30 μM and 100 μM salidroside significantly reversed the adverse effects of DHT (Figure 2E and F).

In general, oxidative stress and other cellular stressors initiate mitochondrial apoptosis via mitochondrial outer membrane permeabilization (MOMP), which involves the release of cytochrome C into the cytoplasm[23]. In the cytoplasm, cytochrome C activates apoptosis mediator caspase-9, which in turn cleaves and activates the executor caspase, caspase-3[24]. This eventually disintegrates cells, followed by cell death. Furthermore, this process is tightly regulated by anti-apoptotic protein Bcl-2 and pro-apoptotic effector protein Bax[25]. Thus, to further determine the effects of salidroside on KGN cells, the levels of these apoptosis-related proteins were assessed. Interestingly, salidroside treatment resulted in a significant decrease in the levels of Bax, cleaved caspase-9, and cleaved caspase-3 in KGN cells as compared to DHT-induced cells. In comparison to these, Bcl-2 levels were found to be reversed upon salidroside treatment (Figure 2G and H). SOD2 is a mitochondrial antioxidant enzyme that removes intracellular ROS and plays a vital role in the maintenance of redox balance[26]. As shown in Figure 2G and H, DHT treatment resulted in a slight increase in SOD2 protein levels, whereas the protein expression levels of SOD2 were significantly enhanced by salidroside (Figure 2G and H).

Salidroside activates Nrf2 pathway in KGN cells

Keap1-Nrf2-antioxidant response element (ARE) signaling pathway plays a pivotal role in the biological response to oxidative stress, via regulation of the transcription of a variety of antioxidant genes[27]. Thus, the effects of salidroside on the Keap1/Nrf2 pathway and its downstream antioxidant proteins in DHT-induced KGN cells were evaluated. The results for western blot analysis indicated that DHT treatment slightly increased the expression of Nrf2, whereas salidroside treatment resulted in significant stimulation of the total Nrf2 protein expression and promoted its nuclear translocation. In concordance with these results, the expression of Keap1 was also restrained after salidroside treatment (Figure 3A–C). Moreover, the immunofluorescence staining results further confirmed the nuclear translocation of Nrf2 (Figure 3D). To evaluate the levels of Nrf2-targeted antioxidant proteins, the protein expression of NQO1 and HO-1 was assessed. As shown in Figures 3E and F, HO-1 and NQO1 were slightly upregulated upon DHT exposure, whereas salidrodide treatment resulted in significant upregulation of these proteins (Figure 3E and F). The aforementioned results indicated that salidroside initiated Nrf2 signaling in KGN cells.

Protective effects of salidroside treatment were blocked by Nrf2 knockdown

To further prove the role of Nrf2 pathway activation in the protective role of salidroside in KGN cells, the cells were transfected with Nrf2 siRNA. The knockdown efficiency of Nrf2 siRNA-3 was found to be ~75% and thus was selected to silence the target gene in the following studies (Figure 4A and B). As shown in Figures 4C and D, the Nrf2 siRNA decreased the total protein levels of Nrf2 and partially prevented the nuclear translocation of Nrf2. Besides this, the silencing of Nrf2 nullified the upregulation of antioxidant protein NQO1 and HO-1 (Figure 4C and D). In addition to this, the levels of the apoptosis-related proteins were also assessed. The results for western blotting analysis showed that the attenuation of Bax, cleaved

caspase-3, and cleaved caspase-9 and upregulation of Bcl-2 and SOD2 were prevented by Nrf2 siRNA supplementation (Figure 4E and F). In concordance with these results, ROS production evaluation by flow cytometry and JC-1 probe staining showed that the protective effects of salidroside on ROS elimination and mitochondrial depolarization in KGN cells were partly reversed by Nrf2 silencing (Figure 4G–J). Treatment with salidroside (60 μM) resulted in a decrease in apoptosis in DHT-exposed KGN cells, while knockdown of Nrf2 nullified this protection (Figure 4K and L).

Effects of salidroside on MAPK and AMPK pathways in DHT-treated KGN cells

Recent studies have reported that AMPK, phosphatidylinositol 3-kinase (PI3K), c-Jun N-terminal kinase (JNK), p38, and extracellular signal-regulated protein kinase (ERK) promote the separation of the Keap-Nrf2 complex and assist in its nuclear translocation[28-31]. To explore the regulatory signaling pathway involved in Nrf2 nuclear translocation, the expression levels of proteins in the MAPK and AMPK pathways were assessed in KGN cells. As shown in Figures 5A and B, salidroside treatment conferred no effect on p-ERK and p-Akt, and a slight increase observed for p-JNK and p-p38. However, these changes were not statistically significant. Importantly, salidroside resulted in a significant increase in the phosphorylation of AMPK in DHT-treated KGN cells (Figure 5A and C). Next, the effect of salidroside on AMPK was examined under different concentration conditions (0, 30, 60, 80, and 100μM). Interestingly, salidroside mediated AMPK activation in a dose-dependent manner (Figure 5D and E).

Involvement of AMPK in salidroside-induced Nrf2 nuclear translocation

To further investigate the role of AMPK in salidroside-induced Nrf2 activation, siRNA molecules specific to AMPK were utilized for a knockdown. The knockdown efficiency of AMPK siRNA-2 was found to be ~65% (Figure 6A and B), and it was selected to silence the target gene in the following studies (Figure 6C–G). The results for western blotting analysis demonstrated that AMPK siRNA prevented the phosphorylation of AMPK and the nuclear translocation of Nrf2 (Figure 6C–E). Besides this, the expression of the downstream antioxidant proteins HO-1 and NQO-1 was found to be inhibited (Figure 6F and G). Next, an AMPK specific inhibitor, Compound C, was used to revalidate the expression of AMPK at the concentration of 10μM as several studies[32]. The obtained results were consistent with the effects of AMPK knockdown (Figure 6H–L). Altogether, the aforementioned data suggested that AMPK is the upstream signaling molecule in the nuclear translocation of Nrf2.

Discussion

Over the past two decades, comprehensive studies have demonstrated that oxidative stress contributes to the initiation and development of pathological processes that impair female reproduction[33]. PCOS is the most common reproductive endocrine disorder in women under reproductive age; however, the pathological mechanism for the same remains unclear. Interestingly, the intrinsic association of PCOS and redox imbalance has been increasingly detected and established in several studies[34]. KGN cell line is considered to be consistent with the immature granulosa cells obtained from smaller antral

follicles, in terms of physiological characteristics[5]. In fact, DHT-induced KGN cells have been widely used as a PCOS model for *in vitro* studies[7]. Salidroside, the main bioactive compound extracted from *Rhodiola*, has been shown to possess a variety of pharmacological activities, including anti-inflammatory, anti-depressive, anti-oxidant, and anti-cancerous activities[19, 35-37]. Recent accumulation of evidence proved that salidroside could alleviate oxidative stress levels. The present study is the first to demonstrate that salidroside could ameliorate apoptosis and oxidative stress in KGN cells, PCOS cell model, via activation of the Nrf2 signaling pathway.

In general, ovarian granulosa cells grow around oocytes and deliver metabolites required for the growth and development of oocytes. Additionally, these cells also participate in the production of estrogen and play a key role in the growth and development of follicles[38]. The accumulation of ROS could possibly cause oxidative stress that might lead to apoptosis in oocytes deteriorating the quality of oocytes, which further affects the fertility outcomes[39]. Recent studies have reported that increased apoptosis and ROS levels in thin granulosa cells participate in the pathogenesis of PCOS, and result in abnormal follicle development and clinical pregnancy[40]. Hence, the present study utilized DHT-induced KGN cells to assess the protective effects of salidroside on the PCOS cell model. First, the survival of KGN cells was tested in the presence of salidroside. Both low and high concentrations of salidroside showed no side effects on the viability of KGN cells and improved the survival inhibition post DHT treatment. In concordance with these results, further functional analyses also showed that salidroside alleviated ROS accumulation, mitochondrial depolarization, and increased apoptosis in KGN cells. Cell apoptosis mediated by mitochondria is initiated by intracellular apoptotic stimulators, like DNA damages and anoxic damage, and regulated mainly by Bcl-2 family proteins, comprising of pro-apoptotic protein Bax and anti-apoptotic protein Bcl-2. Bcl-2 family proteins control cellular apoptosis by regulating MOMP and promoting the release of proteins from intermembrane space into the cytoplasm, which further activates the caspase cascade, resulting in cell death[41]. In the present study, the changes of expression levels of apoptosis-related proteins, namely Bax, Bcl-2, cleaved caspase-3, and cleaved caspase-9 were suggestive of activation of mitochondrial apoptosis in DHT-induced KGN cells and the protective effects of salidroside.

The transcription factor Nrf2 is well established key regulator involved in cellular oxidative stress[42]. Recent studies have reported the protective effects of Nrf2 in various biological processes, including inflammation, autophagy, and unfolded protein response[43-45]. In steady conditions, Nrf2 is mainly located in the cytoplasm at a low basal protein level, mainly due to Keap1 mediated proteasomal degradation. During oxidative stress, electrophiles and ROS inactivate Keap1, resulting in the release of Nrf2 from the Nrf2-Keap1 complex, followed by its nuclear translocation. Post its nuclear accumulation, Nrf2 binds to the antioxidant response element (ARE) and stimulates downstream anti-oxidant proteins, like HO-1 and NQO1[42]. Several studies have previously revealed that salidroside treatment activated Nrf2 in different disease models[22, 46]. In the present study, DHT treatment resulted in a slight increase in Nrf2 protein levels. In comparison to this, salidroside decreased the levels of Keap1 protein, and thus induced a significant increase in Nrf2 levels, further promoting its nuclear translocation. Besides this, the

antioxidant proteins HO-1 and NQO1 were also found to be upregulated after salidroside treatment. Additionally, silencing of Nrf2 resulted in the deterioration of oxidative stress and apoptosis and a partial reversal of the protective effects conferred by salidroside in KGN cells. Altogether, these results demonstrated that salidroside alleviates apoptosis and oxidative stress via upregulation of Nrf2 mediated antioxidant proteins.

It remains unclear which signaling pathway participated in the stimulation of Nrf2. MAPK and AMPK signal pathways have been previously reported to be involved in the upstream signal of Nrf2[47, 48]. AMPK is known as an evolutionarily conserved energy sensor in cellular energy homeostasis. Under oxidative stress, AMPK is actived by the phosphorylation at Thr172 and exerts an antioxidant effect through promoting the transcription of downstream genes such as FoxO factors, DAF-16, Nrf2 and SIRT1[49]. In the present study, phosphorylation of AMPK was found to be upregulated in the case of salidroside treatment. Additionally, AMPK siRNA supplementation partly restrained the stimulation and nuclear translocation of Nrf2. Similarly, the use of an inhibitor of AMPK, Compound C, showed consistent inhibitory effects on Nrf2 activation. Thus, these results indicated that AMPK activated Nrf2 as an upstream signal in salidroside-treated KGN cells. However, Nrf2 activation could be mediated by different pathways. Several studies have previously shown that there are alternative mechanisms for Nrf2 stimulation, independent of Keap1[50]. Besides this, the regulatory factors at the post-transcriptional level like RNA-binding proteins (RBPs) can bind to the 30-UTR of *NFE2L2*mRNA to increase the Nrf2 activation[42, 51]. Thus, other modes of Nrf2 stimulation might be involved in the protective effects conferred by salidroside treatment in KGN cells, which need to be explored in the future.

In summary, the present study for the first time demonstrated that salidroside could restrain apoptosis and oxidative stress in KGN cells under DHT exposure, via AMPK mediated Nrf2 activation. Besides this, these findings are indicative of the therapeutic potential of salidroside for PCOS treatment that should be explored in appropriate *in vivo* models.

Declarations

Ethics approval and consent to participate

Not applicable.

Consent for publication

Not applicable.

Conflict of interest

The authors declare no conflict of interest.

Author contributions

R.J., F.Y.J. and X.C. contributed equally to this work. The study was designed by J.Y., R.J. and F.Y.J., and the experiments in KGN cells were performed by R.J. and X.C. Experimental analysis was performed by R.J., F.Y.J., Z.H.W., W.Y.J. and X.C. The manuscript was written by R.J. and F.Y.J.

Acknowledgement

This work was supported by Reproductive Medical Center, Renmin Hospital of Wuhan University, Wuhan, China.

Funding

This research was supported by the National Natural Science Foundation of China (Grant No. 81971356， 81771662, 81771618) and the National Key Research and Development Program of China (No. 2016YFC1000600， 2018YFC1002804).

Availability of data and materials

The datasets analysed during the current study are available from the author on reasonable request.

References

1. Jaffe LA, Egbert JR. Regulation of Mammalian Oocyte Meiosis by Intercellular Communication Within the Ovarian Follicle. Annu Rev Physiol. 2017;79:237–60.
2. Rehnitz J, Alcoba DD, Brum IS, et al. FMR1 expression in human granulosa cells increases with exon 1 CGG repeat length depending on ovarian reserve. Reprod Biol Endocrinol. 2018;16:65.
3. Dilaver N, Pellatt L, Jameson E, et al. The regulation and signalling of anti-Mullerian hormone in human granulosa cells: relevance to polycystic ovary syndrome. Hum Reprod. 2019;34:2467–79.
4. Dewailly D, Robin G, Peigne M, Decanter C, Pigny P, Catteau-Jonard S. Interactions between androgens, FSH, anti-Mullerian hormone and estradiol during folliculogenesis in the human normal and polycystic ovary. Hum Reprod Update. 2016;22:709–24.
5. Nishi Y, Yanase T, Mu Y, et al. Establishment and characterization of a steroidogenic human granulosa-like tumor cell line, KGN, that expresses functional follicle-stimulating hormone receptor. Endocrinology. 2001;142:437–45.
6. Yi S, Zheng B, Zhu Y, Cai Y, Sun H, Zhou J. Melatonin ameliorates excessive PINK1/Parkin-mediated mitophagy by enhancing SIRT1 expression in granulosa cells of PCOS. Am J Physiol Endocrinol Metab. 2020;319:E91–101.
7. Zhou R, Li S, Liu J, et al. Up-regulated FHL2 inhibits ovulation through interacting with androgen receptor and ERK1/2 in polycystic ovary syndrome. EBioMedicine. 2020;52:102635.
8. Saglam E, Canakci CF, Sebin SO, et al. Evaluation of oxidative status in patients with chronic periodontitis and polycystic ovary syndrome: A cross-sectional study. J Periodontol. 2018;89:76–84.

9. Liu Y, Yu Z, Zhao S, et al. Oxidative stress markers in the follicular fluid of patients with polycystic ovary syndrome correlate with a decrease in embryo quality. J Assist Reprod Genet. 2021;38:471–7.
10. Zhang J, Bao Y, Zhou X, Zheng L. Polycystic ovary syndrome and mitochondrial dysfunction. Reprod Biol Endocrinol. 2019;17:67.
11. Prasad S, Tiwari M, Pandey AN, Shrivastav TG, Chaube SK. Impact of stress on oocyte quality and reproductive outcome. J Biomed Sci. 2016;23:36.
12. Tonelli C, Chio IIC, Tuveson DA. Transcriptional Regulation by Nrf2. Antioxid Redox Signal. 2018;29:1727–45.
13. Kopacz A, Kloska D, Forman HJ, Jozkowicz A, Grochot-Przeczek A. Beyond repression of Nrf2: An update on Keap1. Free Radic Biol Med. 2020;157:63–74.
14. Dinkova-Kostova AT, Abramov AY. The emerging role of Nrf2 in mitochondrial function. Free Radic Biol Med. 2015;88:179–88.
15. Yang H, Lv H, Li H, Ci X, Peng L. Oridonin protects LPS-induced acute lung injury by modulating Nrf2-mediated oxidative stress and Nrf2-independent NLRP3 and NF-kappaB pathways. Cell Commun Signal. 2019;17:62.
16. Zhang Y, Ahmad KA, Khan FU, Yan S, Ihsan AU, Ding Q. Chitosan oligosaccharides prevent doxorubicin-induced oxidative stress and cardiac apoptosis through activating p38 and JNK MAPK mediated Nrf2/ARE pathway. Chem Biol Interact. 2019;305:54–65.
17. Lin SC, Hardie DG. AMPK: Sensing Glucose as well as Cellular Energy Status. Cell Metab. 2018;27:299–313.
18. Song C, Heping H, Shen Y, et al. AMPK/p38/Nrf2 activation as a protective feedback to restrain oxidative stress and inflammation in microglia stimulated with sodium fluoride. Chemosphere. 2020;244:125495.
19. Tang C, Zhao CC, Yi H, et al. Traditional Tibetan Medicine in Cancer Therapy by Targeting Apoptosis Pathways. Front Pharmacol. 2020;11:976.
20. Nabavi SF, Braidy N, Orhan IE, Badiee A, Daglia M, Nabavi SM. Rhodiola rosea L. and Alzheimer's Disease: From Farm to Pharmacy. Phytother Res. 2016;30:532–9.
21. Zheng T, Bian F, Chen L, Wang Q, Jin S. Beneficial Effects of Rhodiola and Salidroside in Diabetes: Potential Role of AMP-Activated Protein Kinase. Mol Diagn Ther. 2019;23:489–98.
22. Zhu Y, Zhang YJ, Liu WW, Shi AW, Gu N. Salidroside Suppresses HUVECs Cell Injury Induced by Oxidative Stress through Activating the Nrf2 Signaling Pathway. Molecules. 2016;21.
23. Bock FJ, Tait SWG. Mitochondria as multifaceted regulators of cell death. Nat Rev Mol Cell Biol. 2020;21:85–100.
24. Budihardjo I, Oliver H, Lutter M, Luo X, Wang X. Biochemical pathways of caspase activation during apoptosis. Annu Rev Cell Dev Biol. 1999;15:269–90.
25. Ladokhin AS. Regulation of Apoptosis by the Bcl-2 Family of Proteins: Field on a Brink. Cells. 2020;9.

26. Cyr AR, Hitchler MJ, Domann FE. Regulation of SOD2 in cancer by histone modifications and CpG methylation: closing the loop between redox biology and epigenetics. Antioxid Redox Signal. 2013;18:1946–55.
27. Bellezza I, Giambanco I, Minelli A, Donato R. Nrf2-Keap1 signaling in oxidative and reductive stress. Biochim Biophys Acta Mol Cell Res. 2018;1865:721–33.
28. Lv H, Liu Q, Wen Z, Feng H, Deng X, Ci X. Xanthohumol ameliorates lipopolysaccharide (LPS)-induced acute lung injury via induction of AMPK/GSK3beta-Nrf2 signal axis. Redox Biol. 2017;12:311–24.
29. Li ST, Dai Q, Zhang SX, et al. Ulinastatin attenuates LPS-induced inflammation in mouse macrophage RAW264.7 cells by inhibiting the JNK/NF-kappaB signaling pathway and activating the PI3K/Akt/Nrf2 pathway. Acta Pharmacol Sin. 2018;39:1294–304.
30. Wong SY, Tan MG, Wong PT, Herr DR, Lai MK. Andrographolide induces Nrf2 and heme oxygenase 1 in astrocytes by activating p38 MAPK and ERK. J Neuroinflammation. 2016;13:251.
31. Zhang H, Liu X, Zhou S, et al. SP600125 suppresses Keap1 expression and results in NRF2-mediated prevention of diabetic nephropathy. J Mol Endocrinol. 2018;60:145–57.
32. Reverchon M, Cornuau M, Cloix L, et al. Visfatin is expressed in human granulosa cells: regulation by metformin through AMPK/SIRT1 pathways and its role in steroidogenesis. Mol Hum Reprod. 2013;19:313–26.
33. Lu J, Wang Z, Cao J, Chen Y, Dong Y. A novel and compact review on the role of oxidative stress in female reproduction. Reprod Biol Endocrinol. 2018;16:80.
34. Mancini A, Bruno C, Vergani E, d'Abate C, Giacchi E, Silvestrini A. Oxidative Stress and Low-Grade Inflammation in Polycystic Ovary Syndrome: Controversies and New Insights. Int J Mol Sci. 2021;22.
35. Xu F, Xu J, Xiong X, Deng Y. Salidroside inhibits MAPK, NF-kappaB, and STAT3 pathways in psoriasis-associated oxidative stress via SIRT1 activation. Redox Rep. 2019;24:70–4.
36. Pu WL, Zhang MY, Bai RY, et al. Anti-inflammatory effects of Rhodiola rosea L.: A review. Biomed Pharmacother. 2020;121:109552.
37. Amsterdam JD, Panossian AG. Rhodiola rosea L. as a putative botanical antidepressant. Phytomedicine. 2016;23:770–83.
38. Eppig JJ. Reproduction. Oocytes Call, Granulosa Cells Connect. Curr Biol. 2018;28:R354–6.
39. Sasaki H, Hamatani T, Kamijo S, et al. Impact of Oxidative Stress on Age-Associated Decline in Oocyte Developmental Competence. Front Endocrinol (Lausanne). 2019;10:811.
40. Lai Q, Xiang W, Li Q, et al. Oxidative stress in granulosa cells contributes to poor oocyte quality and IVF-ET outcomes in women with polycystic ovary syndrome. Front Med. 2018;12:518–24.
41. Kale J, Osterlund EJ, Andrews DW. BCL-2 family proteins: changing partners in the dance towards death. Cell Death Differ. 2018;25:65–80.
42. He F, Ru X, Wen T. NRF2, a Transcription Factor for Stress Response and Beyond. Int J Mol Sci. 2020;21.

43. Jiang T, Harder B, Rojo de la Vega M, Wong PK, Chapman E, Zhang DD. p62 links autophagy and Nrf2 signaling. Free Radic Biol Med. 2015;88:199–204.
44. Ahmed SM, Luo L, Namani A, Wang XJ, Tang X. Nrf2 signaling pathway: Pivotal roles in inflammation. Biochim Biophys Acta Mol Basis Dis. 2017;1863:585–97.
45. Periyasamy P, Shinohara T. Age-related cataracts: Role of unfolded protein response, Ca(2+) mobilization, epigenetic DNA modifications, and loss of Nrf2/Keap1 dependent cytoprotection. Prog Retin Eye Res. 2017;60:1–19.
46. Xu N, Huang F, Jian C, et al. Neuroprotective effect of salidroside against central nervous system inflammation-induced cognitive deficits: A pivotal role of sirtuin 1-dependent Nrf-2/HO-1/NF-kappaB pathway. Phytother Res. 2019;33:1438–47.
47. Jasek-Gajda E, Jurkowska H, Jasinska M, Lis GJ. Targeting the MAPK/ERK and PI3K/AKT Signaling Pathways Affects NRF2, Trx and GSH Antioxidant Systems in Leukemia Cells. Antioxidants (Basel). 2020;9.
48. Tanaka M, Kishimoto Y, Sasaki M, et al. Terminalia bellirica (Gaertn.) Roxb. Extract and Gallic Acid Attenuate LPS-Induced Inflammation and Oxidative Stress via MAPK/NF-kappaB and Akt/AMPK/Nrf2 Pathways. Oxid Med Cell Longev. 2018;2018:9364364.
49. Salminen A, Kaarniranta K. AMP-activated protein kinase (AMPK) controls the aging process via an integrated signaling network. Ageing Res Rev. 2012;11:230–41.
50. Bryan HK, Olayanju A, Goldring CE, Park BK. The Nrf2 cell defence pathway: Keap1-dependent and -independent mechanisms of regulation. Biochem Pharmacol. 2013;85:705–17.
51. Poganik JR, Long MJC, Disare MT, et al. Post-transcriptional regulation of Nrf2-mRNA by the mRNA-binding proteins HuR and AUF1. FASEB J. 2019;33:14636–52.

Figures

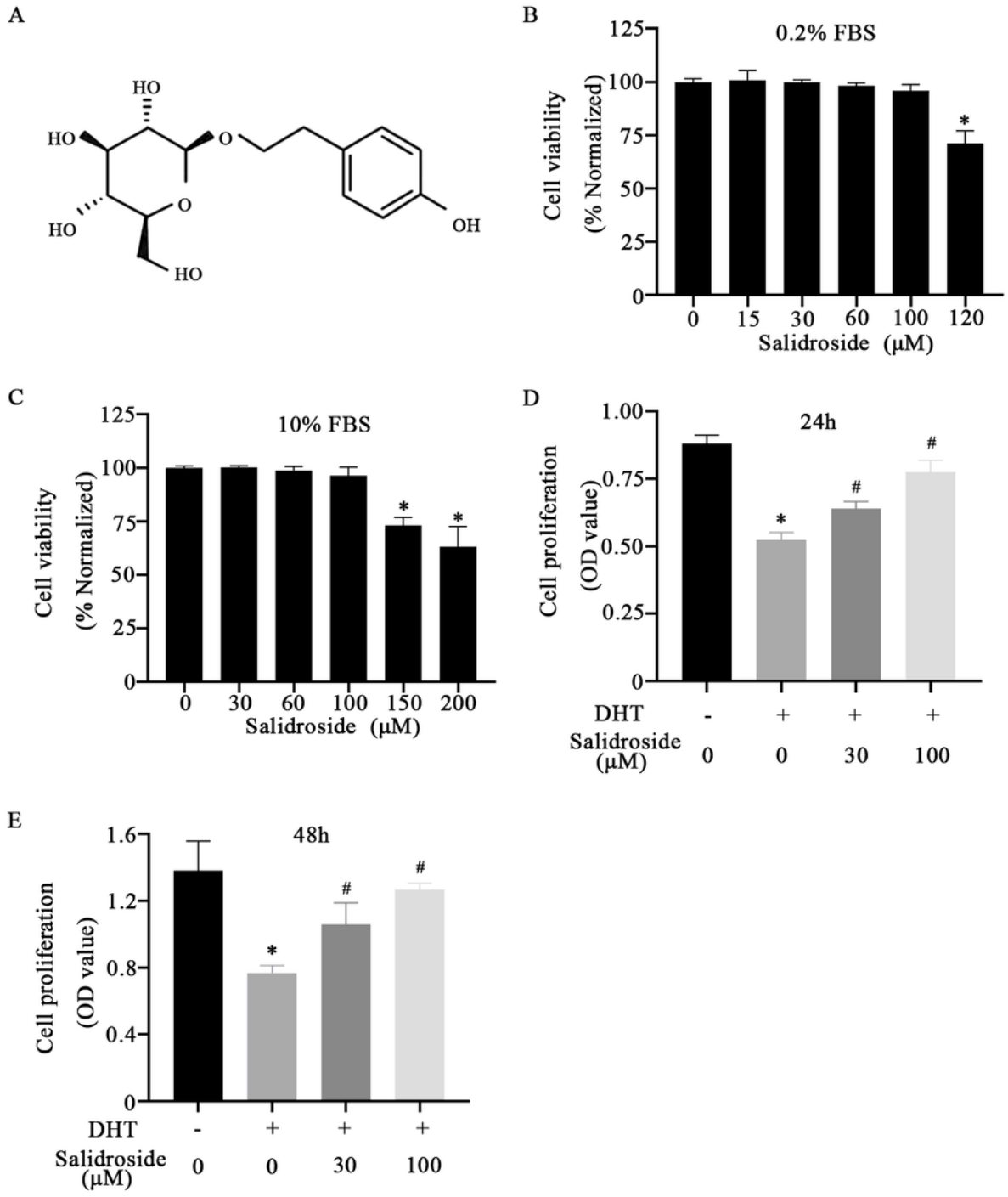

Figure 1

Salidroside improves the survival of DHT-induced KGN cells (A) The chemical structure of carnosol. (B) KGN cells were cultured in DMEM/F12 supplemented with 0.2% FBS in the absence or presence of salidroside (0, 15 μM, 30 μM, 60 μM, 100 μM, and 120 μM) for 24h. (C) KGN cells were cultured in DMEM/F12 supplemented with 10% FBS in the absence or presence of salidroside (0, 30 μM, 60 μM, 100 μM, 150 μM, and 200μM) for 24h. n = 9 for each group. Bars represent mean ± SD. *P□0.05, significantly

different from 0 μM, one-way ANOVA. (D, E) Quiescent KGN cells were incubated with 500nM DHT in the low and high concentration of salidroside for 24 h or 48 h, survival was assessed by the CCK-8 assay. n =9. Bars represent mean ± SD. *P□0.05, significantly different from control, #P□0.05, significantly different from DHT, one-way ANOVA.

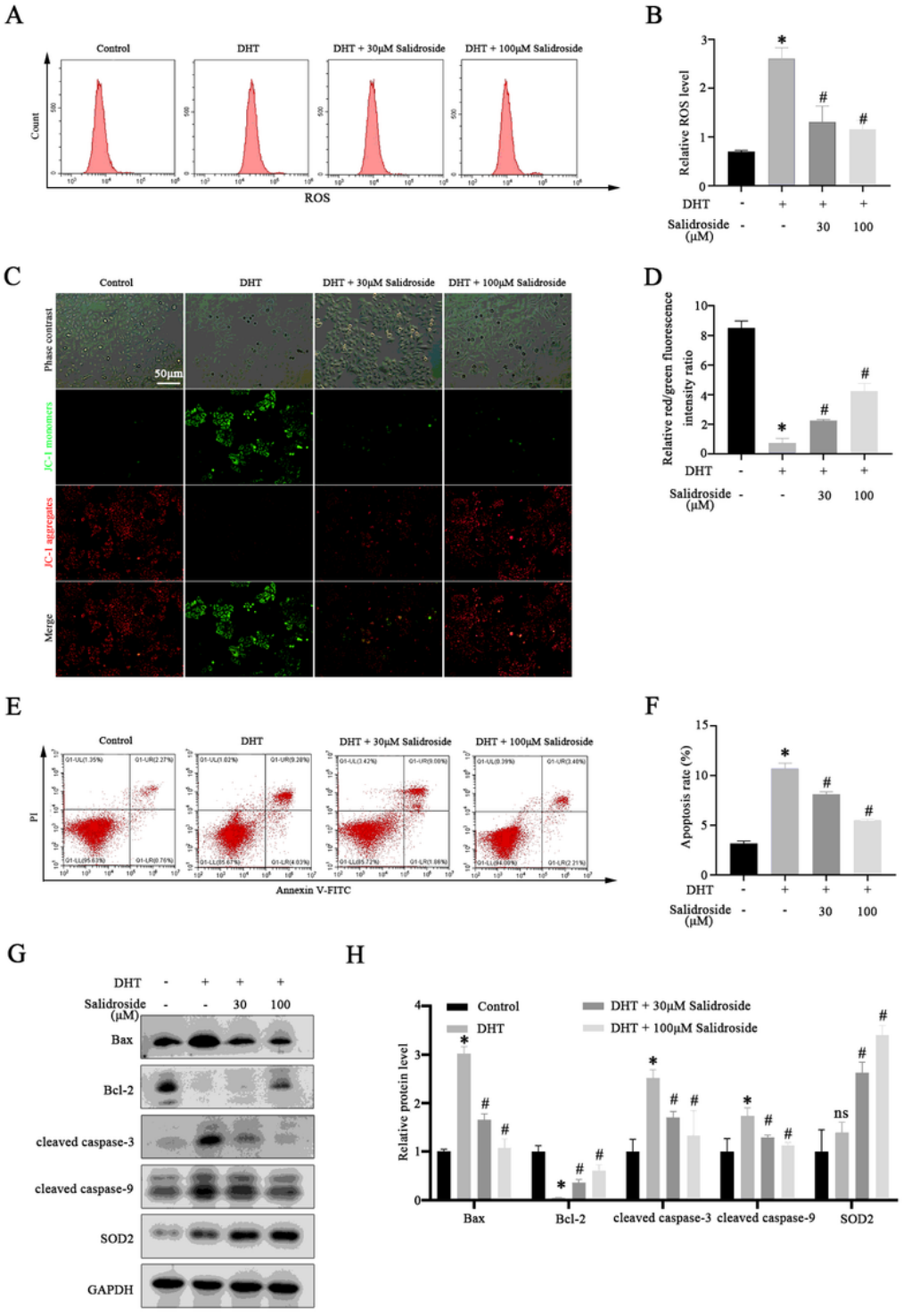

Figure 2

Salidroside alleviates DHT-induced KGN cell apoptosis and oxidative stress (A, B) Effects of salidroside on ROS levels in DHT-treated KGN cells were detected by DHE staining and FCM. (C) Effects of carnosol on mitochondrial membrane potential in DHT-treated KGN cells were measured by JC-1 staining. JC-1 monomers were represented by green fluorescence, while JC-1 aggregates were represented by red fluorescence. (D) Quantitative data of red/green fluorescence intensity ratio in different treatment groups. (E, F) Effects of salidroside on apoptosis in DHT-treated KGN cells were detected by Annexin V-FITC/PI staining and FCM. (G, H) Western blot analysis of the expression of Bax, Bcl-2, cleaved caspase-3, cleaved caspase-9, and SOD2 in KGN cells, normalized to GAPDH. n = 3 for each group. Bars represent mean ± SD. ns, no significant difference from control *P0.05, significantly different from control, #P 0.05, significantly different from DHT, one-way ANOVA.

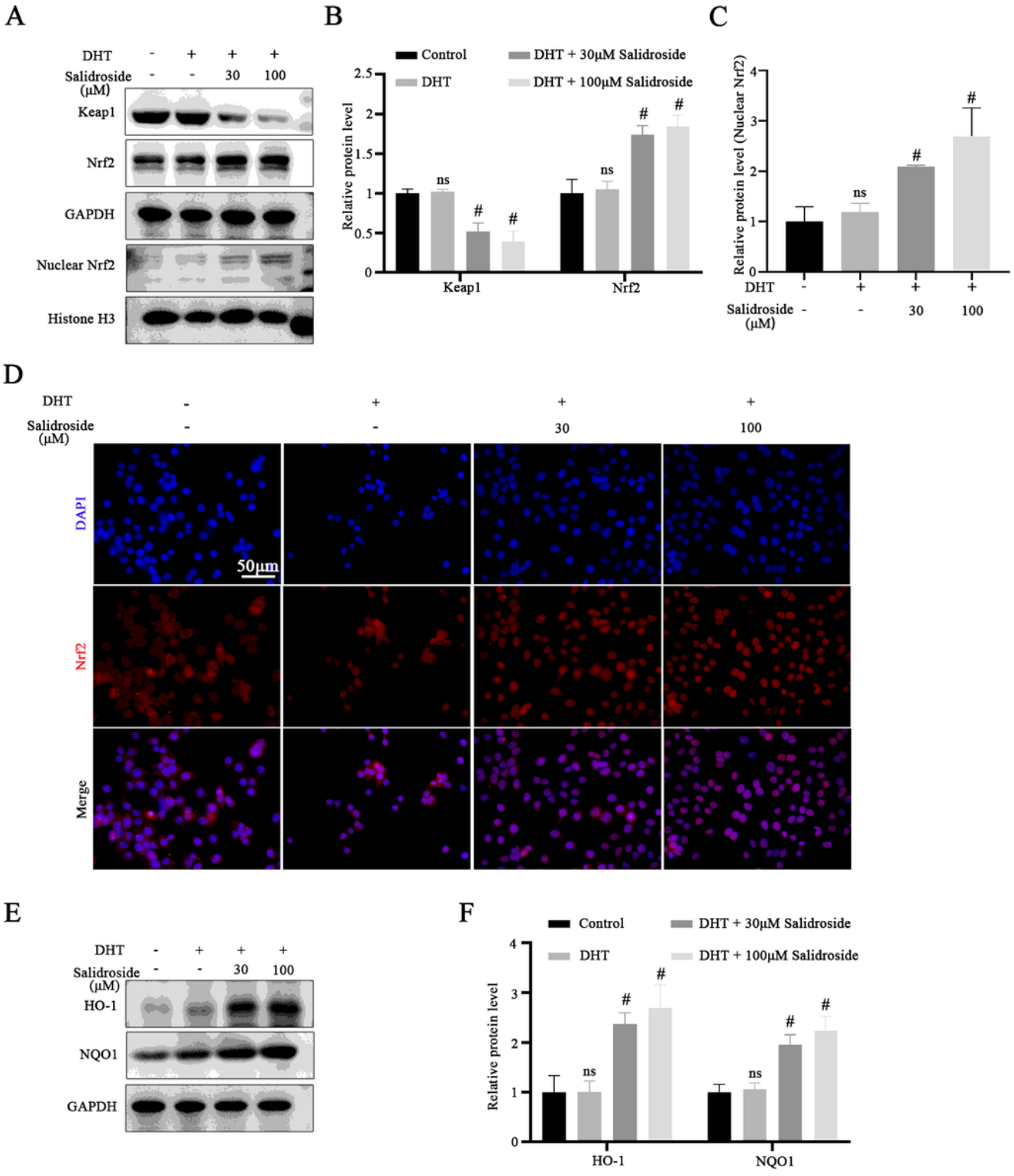

Figure 3

Salidroside activates Nrf2 parthway and upregulates downstream antioxidant proteins in KGN cells (A) Western blotting showing the effects of salidroside on the protein levels of Keap1, total Nrf2 and nuclear Nrf2. (B,C) Relative expression levels of Keap1 and total Nrf2 in KGN cells were normalized to GAPDH, and nuclear Nrf2 expression levels in KGN cells were normalized to Histone 3. (D) Effects of salidroside on the location of Nrf2 in DHT-treated KGN cells measured by immunofluorescent staining. Nuclei were

counterstained with DAPI. (E-F) Expression of HO-1 and NQO1 in KGN cells were detected by western blotting. Relative expression levels of HO-1 and NQO1 in KGN cells were normalized to GAPDH. n=3 for each group. Bars represent mean ± SD. ns, no significant difference from control, #P□0.05, significantly different from DHT, one-way ANOVA.

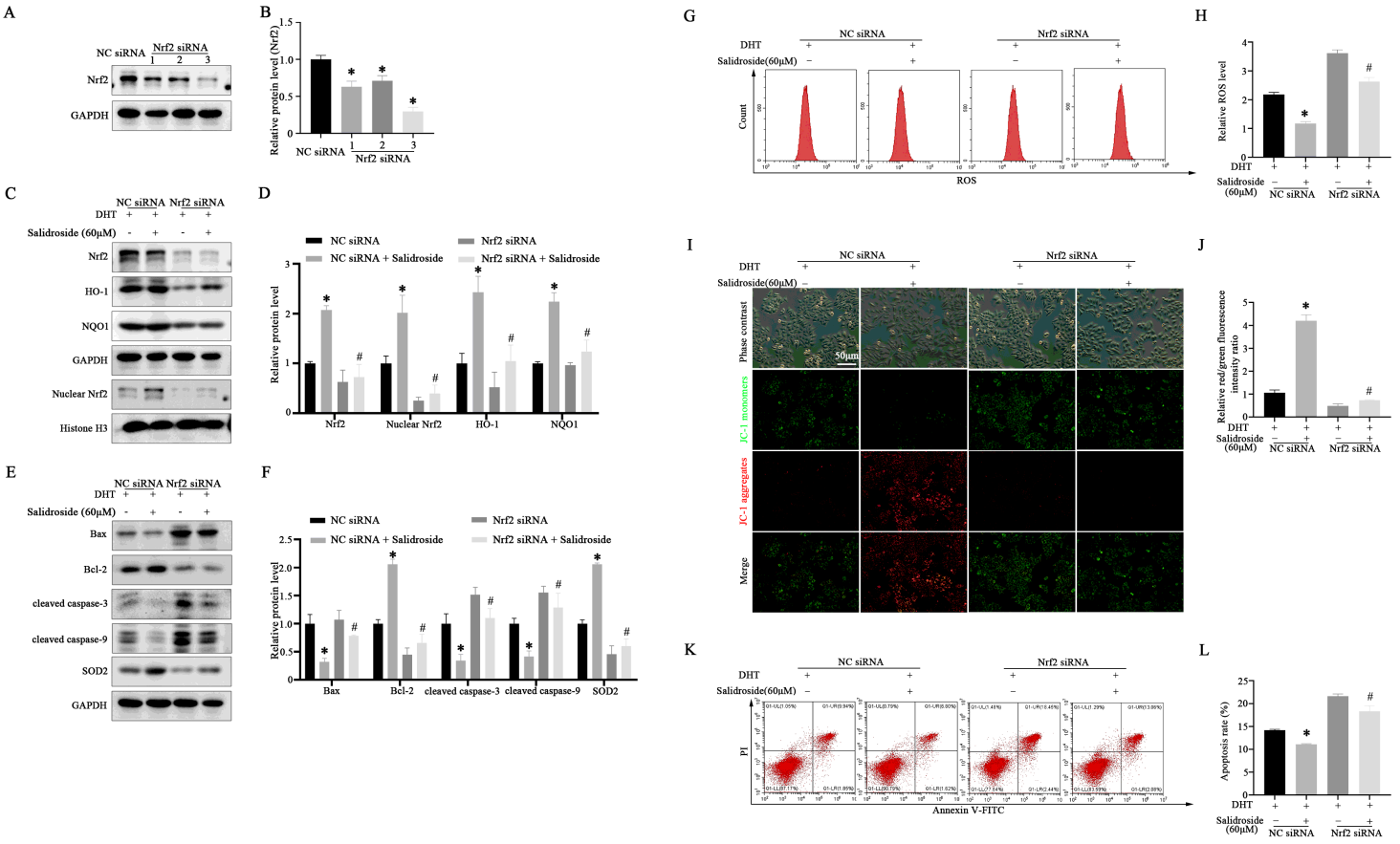

Figure 4

Nrf2 knockdown blocks the protective effect of salidrroside treatment (A, B) Relative expression levels of Nrf2 in KGN cells transfected with NC siRNA or Nrf2 siRNA. n = 3 for each group. Bars represent mean ± SD. *P□0.05, significantly different from NC siRNA, one-way ANOVA. (C-L) DHT-treated KGN cells transfected with NC siRNA or Nrf2 siRNA, followed by 60μM salidroside treatment for 24 h. (C) Representative images showing the protein levels of total Nrf2, nuclear Nrf2, HO-1 and NQO1. (D) total Nrf2, HO-1 and NQO1 expression levels were normalized to GAPDH, nuclear Nrf2 expression level was normalized to that of Histone 3 level. (E, F) Representative images showing the protein levels of Bax, Bcl-2, cleaved caspase-3, cleaved caspase-9, and SOD2 , quantitative data of the relative expression levels were normalized to GAPDH. (G, H) Representative images and quantitative data of the ROS levels in KGN cells were analyzed by DHE staining and FCM detecting. (I) Representative images of JC-1 monomers (green) and aggregates (red) in KGN cells were observed by fluorescence microscopy. (J) Quantitative data of red/green fluorescence intensity ratio in the four groups. (K, L) Representative images and quantitative data of KGN cells apoptosis were detected by Annexin V-FITC/PI staining and FCM detecting.

n = 3 for each group. Bars represent mean ± SD. *P□0.05, significantly different from NC siRNA, #P□0.05, significantly different from NC siRNA + salidroside, one-way ANOVA.

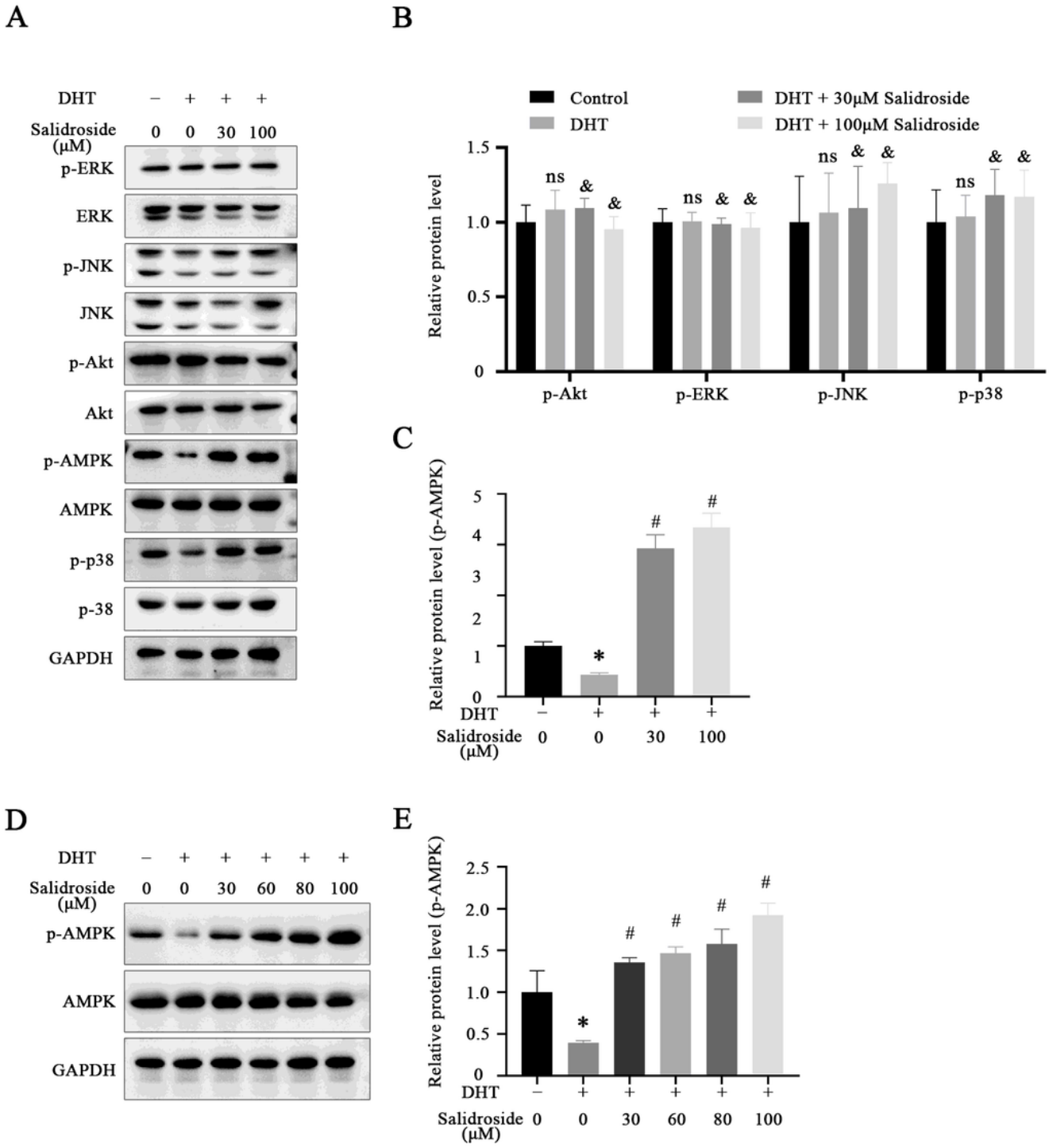

Figure 5

Effects of salidroside on MAPK and AMPK pathway in DHT-treated KGN cells (A-C) Representative western blotting bands and the relative expression levels of ERK, p-ERK, p38, p-p38, JNK, p-JNK, Akt, p-Akt, AMPK and p-AMPK, quantitative data of the relative expression levels were normalized to GAPDH.

(D)Effects of salidroside treatment in different concentrations （0, 30, 60, 80, 100μM）on the protein levels of AMPK and p-AMPK. (E) Quantifications of p-AMPK were performed by densitometric analysis and GAPDH acted as an internal control. n = 3 for each group. Bars represent mean ± SD. ns, no significant difference from control, &, no significant difference from DHT, *P＜0.05, significantly different from control, #P＜0.05, significantly different from DHT, one-way ANOVA.

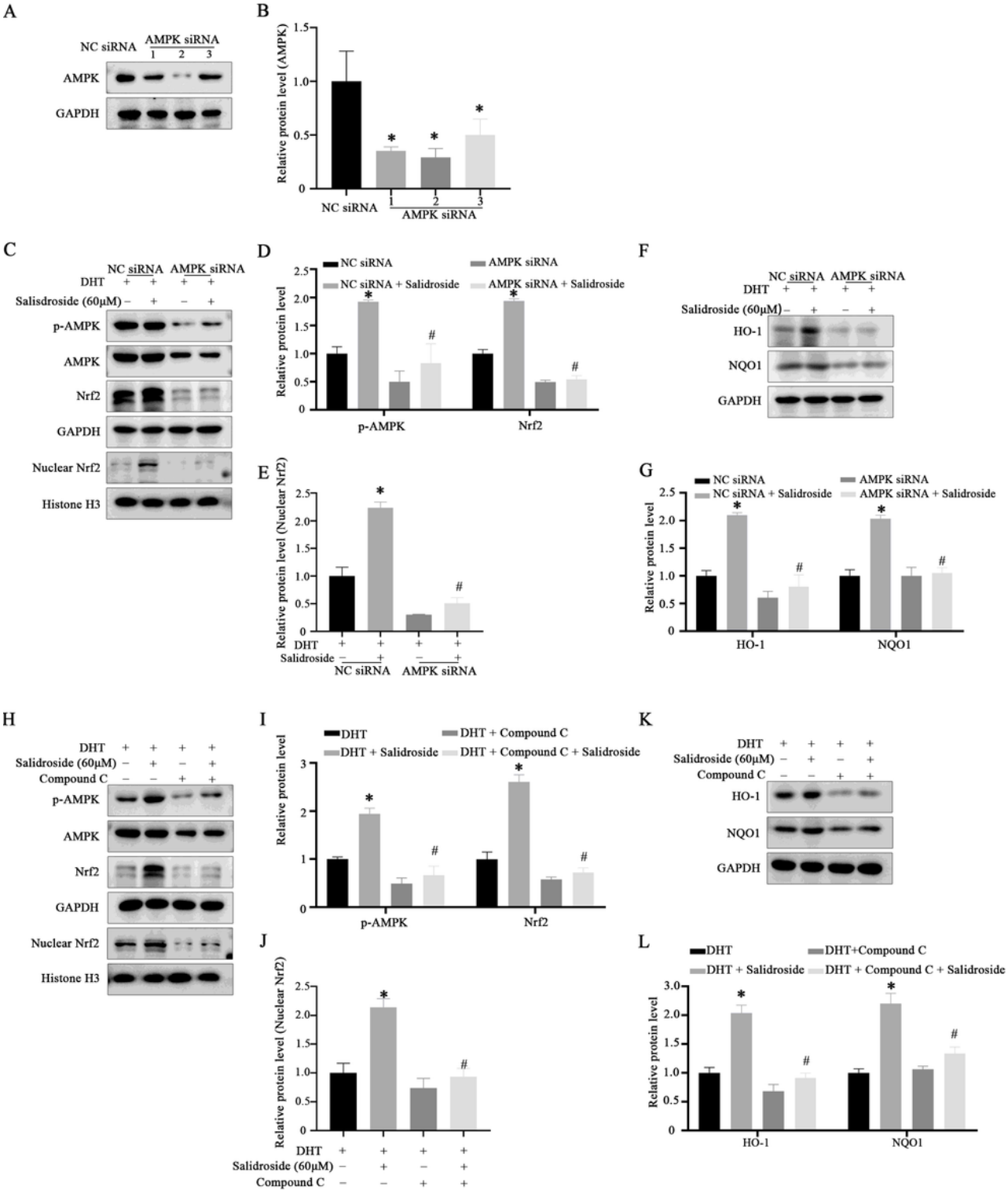

Figure 6

Involvement of AMPK in salidroside-induced Nrf2 nuclear translocation. (A, B) Relative expression levels of AMPK in KGN cells transfected with NC siRNA or AMPK siRNA. n = 3 for each group. Bars represent mean ± SD. *P□0.05, significantly different from NC siRNA, one-way ANOVA. (C-G) DHT-treated KGN cells transfected with NC siRNA or AMPK siRNA, followed by 60μM salidroside treatment for 24 h. (C) Representative images showing the protein levels of p-AMPK, AMPK, total Nrf2 and nuclear Nrf2. (D-E) Protein expression levels of p-AMPK and total Nrf2 were normalized to GAPDH, and nuclear Nre2 levels were normalized to Histone 3. (F-G) Representative images showing the protein levels of HO-1 and NQO1, the protein expression levels were normalized to GAPDH. Bars represent mean ± SD. *P□0.05, significantly different from NC siRNA, #P□0.05, significantly different from NC siRNA+Salidroside, one-way ANOVA. (H-L) KGN cells were pretreated with Compound C (10μM) for 1h, followed by DHT (500nM) and salidroside (60 μM) treatment for 24 h. (H) Representative western blotting bands and the relative expression levels of p-AMPK, AMPK, total Nrf2 and nuclear Nrf2. (I-J) protein expression levels of p-AMPK and total Nrf2 were normalized to GAPDH, and nuclear Nre2 levels were normalized to Histone 3. (K-L) Representative western blotting bands and the relative expression levels of HO-1 and NQO1, the protein expression levels were normalized to GAPDH. n = 3 for each group. Bars represent mean ± SD. *P□0.05, significantly different from control, #P□0.05, significantly different from DHT, one-way ANOVA.